

Design and development of a rheometer for biological fluids of limited availability

A. Scorza, L. Battista, S. Silvestri, and S. A. Sciuto

Citation: [Review of Scientific Instruments](#) **85**, 105105 (2014); doi: 10.1063/1.4897490

View online: <http://dx.doi.org/10.1063/1.4897490>

View Table of Contents: <http://scitation.aip.org/content/aip/journal/rsi/85/10?ver=pdfcov>

Published by the [AIP Publishing](#)

Articles you may be interested in

[The bucket rheometer for shear stress-shear rate measurement of industrial suspensions](#)

J. Rheol. **51**, 821 (2007); 10.1122/1.2750657

[Ultrasonic interferometric sensor for rheological changes of fluids](#)

Rev. Sci. Instrum. **77**, 084902 (2006); 10.1063/1.2336771

[Investigation of the elongational behavior of polymer solutions by means of an elongational rheometer](#)

J. Rheol. **46**, 507 (2002); 10.1122/1.1445185

[How to extract the Newtonian viscosity from capillary breakup measurements in a filament rheometer](#)

J. Rheol. **44**, 653 (2000); 10.1122/1.551105

[The Effects of Temperature and Pressure on the Dynamic Longitudinal Volume Viscosity of Two Model Polymers](#)

J. Rheol. **32**, 533 (1988); 10.1122/1.550000



NEW
Model PS-100
Tabletop Cryogenic
Probe Station



*An affordable solution for
a wide range of research*

Design and development of a rheometer for biological fluids of limited availability

A. Scorza,^{1,a)} L. Battista,² S. Silvestri,³ and S. A. Sciuto¹

¹Department of Engineering, Roma TRE University, via della Vasca Navale 79/81, 00146 Roma, Italy

²Clinical Engineering Service, Religious General Hospital "F. Miulli," Acquaviva delle Fonti (BA), Italy

³Unit of Measurements and Biomedical Instrumentation, Center for Integrated Research, University Campus Bio-Medico of Rome, Via Alvaro del Portillo 21, 00128 Roma, Italy

(Received 25 July 2014; accepted 28 September 2014; published online 13 October 2014)

From studies on the dynamic characterization of human bones, it is noticed that reference data on the viscous behavior of the bone marrow are quite poor. Dependently from marrow limited availability and its opacity, we have not been able to retrieve a tool of appropriate characteristics able to measure bone marrow viscosity. Therefore, principal techniques for the viscosity measurement have been preliminarily examined, and a device suitable for viscosity measurements of biological fluids has been realized. In particular, a rotational rheometer has been developed: it is a coaxial cylinders system, where the fluid flows dragged by the inner cylinder. The device is an absolute rheometer, that is, particularly useful as nowadays it is not known the classification of the bone as far as it concerns its viscous behavior. In this work a preliminary evaluation of the metrological characteristics of the measurement system has been carried out and its main metrological performances have been evaluated.

© 2014 AIP Publishing LLC. [<http://dx.doi.org/10.1063/1.4897490>]

I. INTRODUCTION

Viscosity measurements are important in the study of the fluids flow, as it regards the flow in ducts (i.e., for industrial application) and, generally, the interaction with surfaces (i.e., lubrication, painting).^{1,2} Both these conditions are decisive for the development of physical models to describe the mechanical behavior of bones: in particular, viscosity of the bone marrow seems to be a critical parameter for the normal physiological behavior of bones and a possible indicator of musculoskeletal disorders, that can be used with other diagnostic techniques for health assessment (e.g., electromyography,³ MRI,⁴ etc.). Nevertheless, the measurement of marrow viscosity is particularly difficult, due also to the limited availability of material and the relative low viscosity: these difficulties make the development of specific measuring tools often expensive and complex to manage.

Other difficulties are related to fluid dynamics. A real fluid, in motion, is subjected to stresses along normal and tangential direction. The tangential stress τ (shear stress) is produced when a flow is established. The simplest and more studied model is the motion of a fluid between two parallel and adjacent plates of endless dimensions (Couette), set to a distance $y = h$ and one of them travels with a constant speed U parallel to the other plate that is motionless. In the simplest case the speed profile $u = u(y)$ is linear with shear rate $\gamma = U/h$. As well known, the dynamic viscosity μ is the resistance of particles in a fluid to flow one upon the others: tangential stresses rise up between adjacent layers of fluid when they slide one each other. The relationship between tangential

stresses and μ is described by the Newton law:

$$\tau = \mu \cdot \frac{du}{dy} = \mu \cdot \gamma. \quad (1)$$

In Eq. (1) shear stress τ depends on the dynamic viscosity μ and the shear rate $\gamma = du/dy$. In Newtonian fluids μ is independent from γ but it depends on temperature and pressure, as in a less noticeable way. Other factors^{4,5} that influence the μ value are the chemical nature of the fluid, the electromagnetic field in which the fluid is flowing and the rheologic history. Viscosity is measured in Pa s or in poise, P, where 1 Pa s is equal to 10 P. In these unities the viscosity of the water at 20 °C is almost equal to 1 mPa s = 1 cP. For non-Newtonian fluids (e.g., Bingham-Green fluids, Herschel-Bulkley fluids, pseudoplastic fluids, dilatancy fluids, thixotropic fluids) the relationship between shear stress τ and shear rate γ is not linear, therefore the viscosity is not constant but changes depending on the fluid, as shown in Fig. 1. Instruments used for viscosity measurements are called rheometers or viscometers and they allow to study the rheological behavior in fluids, for a wide range of values: e.g., from water (1 mPa s at 20 °C), honey (1500 mPa s at 20 °C), up to glasses (e.g., 10⁶ mPa s at 1000 °C), evaluating the fluid characteristics at different shear rates, usually between 0.01 and 5000 s⁻¹. The principal methods for measuring rheological characteristics of fluids⁷⁻⁹ can be classified into the followings three categories: (a) capillary techniques, where the viscosity is calculated from the flow measurement and the correspondent pressure drop within a duct; (b) rotational techniques, where one element of the measuring system geometry is rotated and the torque required is measured: viscosity is calculated from the simultaneous measurements of torque and angular speed of the rotor, in steady state conditions; (c) falling sphere techniques, where the viscosity value is deduced from the time a sphere needs to cover a specific distance in the fluid.

^{a)} Author to whom correspondence should be addressed. Electronic mail: andrea.scorza@uniroma3.it

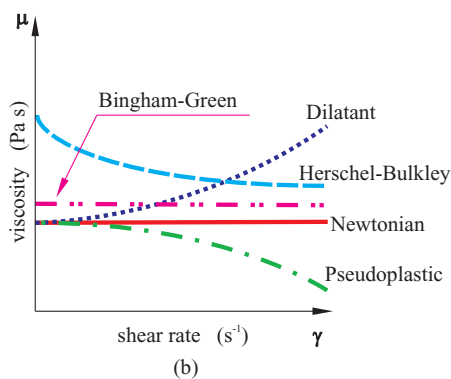
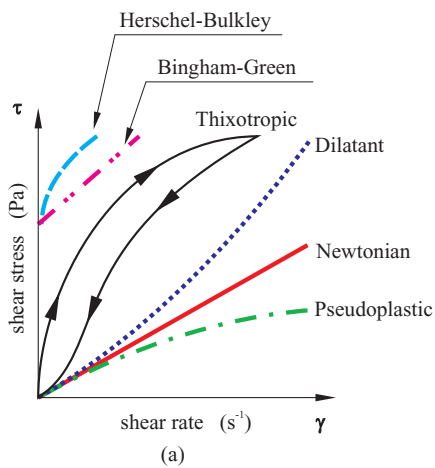


FIG. 1. Rheological curves for different fluids: (a) shear stress versus shear rate; (b) viscosity versus shear rate.

In order to evaluate the more suitable measurement technique, in our work, the following requirements have been examined: fluid properties, availability of the fluid, accuracy of the measurement, frequency of use. Referring to the properties of the human bone marrow¹⁰ (a) the low availability of biological material, (b) its opacity, (c) rheological characteristics, and (d) the unknown value of viscosity under normal conditions of work due to the lack of bibliographical information on its rheological characteristics, we found in rotational rheometers some advantages: versatility, wide measurement range, operative work in a wide temperature and shear rate range, compatibility with Newtonian and non-Newtonian fluids. Moreover, a correct design of the interstice geometry can reduce the amount of fluid needed for the measurement. Main geometries in the scientific literature^{5–12} refer to coaxial cylinders (Fig. 2), to parallel dishes and to cone-flat, also available as interchangeable equipment on the same rheometer. Other available geometries (for laboratory uses) are helices of different forms: disk, shovels, T bar, sphere, spiral, and others.

Among rotational devices, coaxial cylinders instruments (Fig. 2) have generally a lower measurement uncertainty, from 0.5% of full scale range up to approximately 4.0%, whereas rheometers with double interstice geometry are particularly useful in the measurement of very low viscosity liquids (down to 0.01 mPa s) but can be less accurate. Rotational methods provide an absolute value of viscosity, evaluated from the resistance opposed by the fluid to the rotation of a rigid body

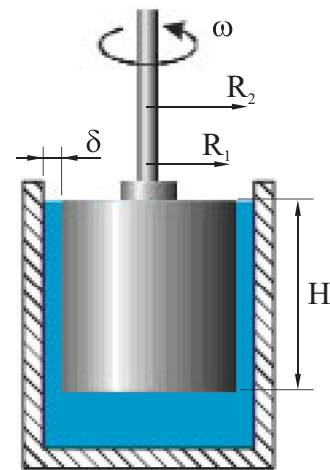


FIG. 2. Coaxial cylinders geometry of a rotational rheometer.

but not depending on equipment settings. In rotational viscometers an electric motor makes a well shaped rotor to move within the fluid in examination. A resistant momentum is provided by the viscous resistance to rotation therefore, viscosity can be evaluated from a momentum measurement. The measurement range, measurement uncertainty and versatility (fluids with particles, organic fluids, small volumes, etc.), charge on the cost of the device. Referring to previous pages, the aim of this work is to show main features of design, development and testing of a low cost rotational rheometer, specific for the viscous behavior characterization of organic fluids and with metrological characteristics that are suitable for research purposes.

II. THEORETICAL MODEL AND EXPERIMENTAL SET-UP

The measurement device is a rotational rheometer with coaxial cylinders in relative motion, where the fluid under test flows between them (Fig. 3). The shear stress τ is due to the rotation of the inside cylinder (rotor) while the external one (container) is motionless under steady state conditions. In Figure 3(a) a zoom of the rotor and the external part is shown, a picture of the whole device is depicted in Figure 3(b). As it

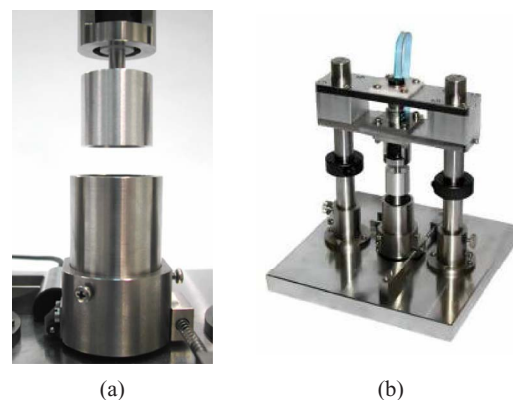


FIG. 3. Rheometer pictures: (a) the rotor (up) extracted by the outer cylinder (down); (b) image of the assembled device.

is known, the shear rate γ is not linear in the interstice (gap) among the two cylinders: it depends on dimensions of cylinders as well on the gap δ , nevertheless, for low values of δ the shear rate can be considered linear, as in Eq. (2):

$$\gamma = \frac{du}{dy} \cong \frac{u_{r=R_1}}{\delta} = \frac{\omega \cdot R_1}{R_2 - R_1}, \quad (2)$$

where R_1 is the outer radius of the rotor, R_2 the inner radius of the container, and ω the angular speed of the rotor. According to standards in bibliography,^{5,12} the height of the cylinders H should be at least 10 times greater the gap δ , and moreover $R_2/R_1 \leq 1.1$.

Using cylindrical coordinates (r, θ, z) , where z is the outer cylinder axis, r is the distance from that axis and θ is the angle in a normal plane to z , for a Newtonian fluid $u(r)$ is the vector speed of the fluid. If the motion is purely circumferential and steady, neglecting effects in the extremities of the device (due to the adherence or the possible presence of a free surface) and for the rotational symmetry:

$$u(r) = (0, u_\theta(r), 0). \quad (3)$$

The circumferential component u_θ of the speed satisfies the equation of continuity and from the Navier-Stokes equation, under condition of fluid adherence to each cylinder surface, an equation system can be formulated:

$$\begin{aligned} \frac{d^2 u_\theta}{dr^2} + \frac{1}{r} \frac{du_\theta}{dr} - \frac{u_\theta}{r^2} &= 0, \\ u_\theta(r = R_1) &= \omega \cdot R_1, \\ u_\theta(r = R_2) &= 0. \end{aligned} \quad (4)$$

From Eq. (4) the solution of u_θ can be determined:

$$u_\theta = \frac{c_1}{r} + c_2 \cdot r = \omega \cdot \frac{R_1^2}{r} \cdot \left(\frac{R_2^2 - r^2}{R_2^2 - R_1^2} \right). \quad (5)$$

Due to the inner cylinder motion and to the viscous force, the shear stress τ_2 on the inner surface of the outer cylinder ($r = R_2$) is

$$\tau_2 = \mu \cdot \left(\frac{du_\theta}{dr} - \frac{u_\theta}{r} \right) \Big|_{r=R_2} = -2\mu \cdot \omega \cdot \left(\frac{R_1^2}{R_2^2 - R_1^2} \right). \quad (6)$$

From τ_2 the viscous force F_{V2} is evaluated for an elementary surface of the outer cylinder $dS_2 = H \cdot (R_2 d\theta)$:

$$\begin{aligned} F_{V2} &= \int_0^{2\pi} \tau_2 \cdot dS_2 = \int_0^{2\pi} \tau_2 \cdot H \cdot R_2 d\theta, \\ F_{V2} &= -2\mu \cdot \omega \cdot \left(\frac{R_1^2}{R_2^2 - R_1^2} \right) \cdot H \cdot R_2 \cdot 2\pi. \end{aligned} \quad (7)$$

The viscous force F_{V2} produces a momentum M_{V2} :

$$M_{V2} = |F_{V2} \cdot R_2| = 4\pi \cdot H \cdot \mu \cdot \omega \cdot \left(\frac{R_1^2 \cdot R_2^2}{R_2^2 - R_1^2} \right). \quad (8)$$

TABLE I. Angular speed limit due to Re and Ta number.

μ (mPa s)	$\omega_{\max \text{ Re}}$		$\omega_{\max \text{ Ta}}$	
	(rad/s)	(rpm)	(rad/s)	(rpm)
1	226	2160	65	621
2	452	4318	130	1242
5	1130	10796	325	3105
10	2260	211600	650	62100

From Eq. (8) the dynamic viscosity μ can be determined. It should be pointed out that the motion is circumferential if instability does not arise because of Taylor vortices, uniformly distributed along the axial direction in the gap. In particular the instability arises for a critical value of the Taylor number (Ta)¹³ and Reynolds number (Re), both of them give a constraint on the angular speed range:

$$\text{Ta} = \left[\frac{\omega \cdot R_1 \cdot (R_2 - R_1)}{v} \right]^2 \cdot \left[\frac{(R_2 - R_1)}{R_1} \right]^2. \quad (9)$$

In Eq. (9) v is the kinematic viscosity (ratio between dynamic viscosity μ and fluid density). If the gap, δ , between cylinders is small in comparison to the radius R_1 of the inner cylinder, a critical value for Ta can be experimentally evaluated¹³ depending on μ : in particular, assuming $\text{Ta} \leq 1708$ and $\mu = 1$ mPa s a constraint can be defined on the maximum angular speed value $\omega_{\max} \leq 65$ rad/s (621 rpm) above which the device does not work correctly. Moreover, the transition from laminar to turbulent flow occurs depending on the Reynolds number $\text{Re} = \rho Lu/\mu$, where ρ is the fluid density, L is a characteristic length dimension (here $L = \delta$), u is the fluid speed, μ is the dynamic viscosity. In the present work a critical value of reference $\text{Re} = 2300$ is calculated: for $\mu = 1$ mPa s another constraint on the angular speed value is determined, $\omega_{\max} \leq 226$ rad/s (2160 rpm). Nevertheless, from bibliography⁸ bone marrow viscosity in humans could have values in the range of about 40 cP (at 36 °C) to about 140 cP with a coefficient of variation up to 0.40 within subjects¹⁴ and therefore, the above speed limit due to Ta and Re could be too restrictive, in Table I other speed limits for ω are shown for different μ values.

Speed values in Table I have to be fitted with maximum torque (Eq. (8)) and working characteristics of suitable electric motors, as shown we found a more restrictive limit on ω_{\max} due to Ta than to Re. Referring to bibliography and to information from Orthopedic surgeons, a measurement range of viscosity among 1 and 100 mPa s has been initially established for the rheometer, this range can be easily extended up to 10 000 mPa s. The measurement range, the small volume of available fluid, limited to 5 cm³, as well as the fluid-dynamic constraints on Ta and Re, determine the dimensions of the two coaxial cylinders through a numerical simulation: the inside diameter $D_2 = 2R_2 = 27.00 \pm 0.01$ mm of the outer cylinder has been evaluated, as well as the diameter $D_1 = 2R_1 = 25.40 \pm 0.01$ mm of the inner rotating cylinder (Fig. 3(a)); the base of the rotating element is hollowed out to reduce its interaction with the fluid (Ekman effect). The rotor is supplied by an electric dc micro-motor Escap 17N78-216E (3.2 W), which

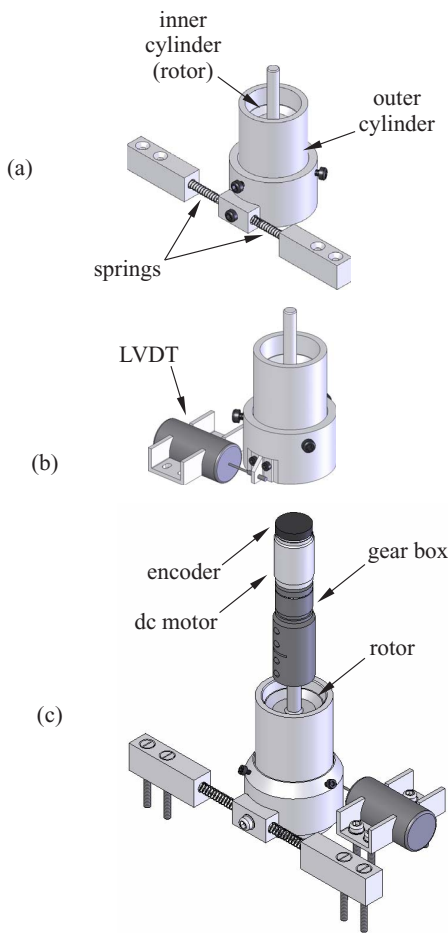


FIG. 4. Details of the rheometer developed: (a) opposing springs and (b) LVDT applied to the outer cylinder; (c) measurement system.

is able to develop a maximum torque of 12.5 mNm and a maximum speed of 8500 rpm. As shown in Fig. 4, the outer cylinder is connected to a rotating support assembled on a radial pad. Since the maximum angular speed of the micro-motor is excessive for our application, a speed reduction gear has been added, with reduction factor of 5.5:1, and an 85% output between the rotor and the micro motor. This solution provides shear rates between 100 and 3000 s^{-1} , with an angular speed of the rotor from 55 to 1650 rpm, respectively. Angular speed ω is measured by a 16 impulses magnetic encoder on the shaft of the electric micro-motor. Under the electric motor action, the fluid flows in the gap and drags the external cylinder: to prevent the free rotation of the outer cylinder, a resistant momentum is applied through a mechanical system, assembled with two compression springs in opposed position (Fig. 4), so the initial force to make the outer cylinder to rotate is minimal.

The measurement of the outer cylinder rotation from the initial configuration is provided by means of a Linear Variable Differential Transformer (LVDT), whose core is rigidly connected to the outside, as shown in Fig. 4. The LVDT measurement range is up to 1 mm and its sensitivity is 780 mV/mm. To ensure a linear output of the LVDT, the rotation of the external cylinder is limited to 1.5° , adopting a system of opposing springs with rigidity equal to 0.16 N/mm (uncertainty below

2%); so the arc of rotation of the external cylinder can be approximated with the tangent of the angle. The output voltage V_{LVDT} from LVDT is proportional to the core displacement Δx , according to $V_{LVDT} = \beta \cdot \Delta x$. Besides, the displacement Δx is determined by the equilibrium between the momentum M_{V2} from the viscous forces and the resistant momentum $M_R = F \cdot b$ from the elastic force $F = k \cdot \Delta x$, where k is the springs stiffness, and b is the distance of the spring joint from the rotation axis of the outer cylinder. From the equilibrium between M_{V2} and M_R in Eq. (10):

$$M_{V2} = M_R, \quad (10)$$

$$4\pi \cdot H \cdot \mu \cdot \omega \cdot \left| \left(\frac{R_1^2 \cdot R_2^2}{R_2^2 - R_1^2} \right) \right| = k \cdot \frac{V_{LVDT}}{\beta} \cdot b.$$

From Eq. (10) the viscosity μ can be calculated:

$$\mu = \frac{\frac{k}{\beta} \cdot b}{4\pi \cdot H \cdot \left| \left(\frac{R_1^2 \cdot R_2^2}{R_2^2 - R_1^2} \right) \right|} \cdot \frac{V_{LVDT}}{\omega} = G_1 \cdot \frac{V_{LVDT}}{\omega}, \quad (11)$$

where G_1 is a constant depending on the geometric and metrological device characteristics:

$$G_1 = \frac{\frac{k}{\beta} \cdot b}{4\pi \cdot H \cdot \left| \left(\frac{R_1^2 \cdot R_2^2}{R_2^2 - R_1^2} \right) \right|}. \quad (12)$$

According to Eq. (11), μ is measured from the angular speed (from encoder) and the output voltage of the LVDT, under steady conditions. If the fluid is Newtonian, the value of μ is the same for every value of rotor speed ω . If the fluid is not-Newtonian, the value of μ depends on ω because it is a function of the shear rate γ , so in a diagram $\tau = \tau(\gamma)$ μ can be calculated as the tangent of the best fit curve. In particular, while the value of γ can be evaluated from the measurement of ω according to Eq. (2), the shear stress results $\tau = G_2 \cdot V_{LVDT}$, with G_2 a constant that depends only on geometrical and metrological characteristics.

III. DEVICE CHARACTERIZATION AND PRELIMINARY RESULTS

For the device validation, experimental diagrams are plotted for four reference Newtonian fluids, with known rheological properties. Angular speed signal V_ω from the encoder and voltage V_{LVDT} from the LVDT core displacement have been collected by a NI data acquisition device (DAQcard) PCI-6062E and processed with LabVIEW software (National Instruments) on a personal computer. Moreover, in order to set the shear rate (electric motor speed) a control has been provided by means of a voltage power amplifier (VPA) managed by the PCI-6062E and LabVIEW software. A type K thermocouple with electronic compensation has been used for fluid temperature measurement. A scheme of the complete measurement setup is shown in Fig. 5.

The viscosity value is obtained by driving the electric motor (voltage steps, Fig. 6) and measuring V_ω and V_{LVDT} in steady state condition, after temperature of the fluid in the outer cylinder has been measured. For each angular speed ω , data acquisition does not start until the steady state conditions

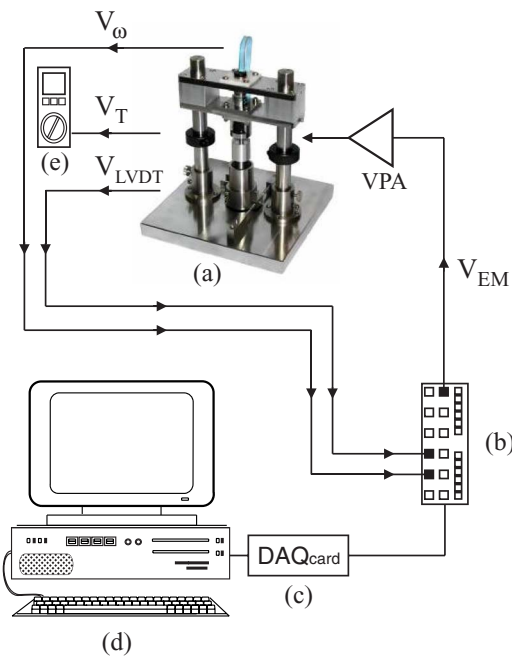


FIG. 5. Measurement set up. (a) Rheometer, (b) NI BNC-2120 shielded connector, (c) DAQ card PCI-6062E, (d) personal computer, (e) multimeter for temperature measurement (type K thermocouple with electronic compensation). Power supplies for instrumentation are not shown.

are reached, after that voltages from the device transducers are processed through LabVIEW software, to get τ and μ values. A preliminary performance characterization has been carried out from the comparison of measurements above with the viscosity value of four reference fluids (Table II).

Equations (10) and (11) are approximated because they do not consider that the rotor has an inferior surface: in particular its base is affected by resistance forces during the rotation,^{3,8,9,15} whose contribution adds to those produced in the gap between the two cylinders. Therefore, an incorrect measurement of the resistant momentum as well as an error on viscosity is made: to fix it, some changes in the geometry of the rotor have been made and a corrective factor to the height H of the interstice (immersion depth) has been determined, so the measured resistant momentum corresponds to an “effective” dimension H' of the depth of immersion. In the present work, the base of the rotor has been modified as shown

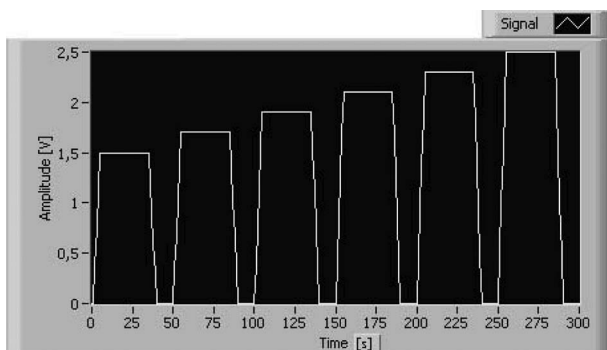


FIG. 6. Voltage steps supplied to the motor. Each step is related to a single angular speed value and shear rate.

TABLE II. Reference fluids characteristics.

Fluid code ^a	Certified viscosity ^b (mPa s)	Relative uncertainty ^{b,c} (%)
5	4.80	1%
10	9.60	1%
50	47.6	1%
100	98.0	1%

^aFluids are made of polydimethylsiloxane mixtures (silicon-based organic polymers).

^bAt 25 °C.

^cWith 95% confidence level.

in Fig. 7(a) and in Eq. (11) the immersion depth H has been increased of a corrective factor H_C , evaluated with the mineral oil Wlodoil SAE 90 (Table III) as below.

In particular, measurements of the resistant moment M_{V2} have been done, making the rotor to dip progressively into the fluid and so increasing the immersion depth H , in correspondence of three different angular speeds (8 rad/s, 17 rad/s, and 26 rad/s). Results have been plotted in the graphs of Fig. 7(b), where they show a dependence of the resistant momentum on the submerged part of the rotor, expressed by an “effective” height of the submerged rotor. In Fig. 7(b), the intercept of each best fit curve (H, M_{V2}) determines the resistant momentum due to rotor base: the corrective factor H_C is calculated from the intersection of best fit curves with the horizontal axis ($M_{V2} = 0$), and in this work it is equal to 2.5 ± 0.4 mm. Such a value provides a correction to the real height H of the dipped rotor so that in the analytical relationships (Eqs. (10) and (11)) a value of effective height $H' = H + H_C$ is used.

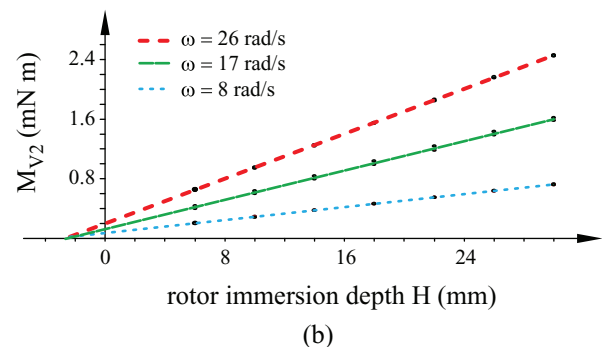
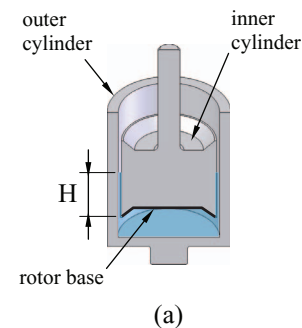


FIG. 7. Elkmann effect compensation and corrective factor H_C . (a) Section of rotor and outer cylinder: a cavity is built in the base of the rotor to minimize the resistances due to the Elkmann effect. (b) Experimental diagrams of the resistant momentum as a function of the immersion depth H of the rotor, for three different angular speeds. The corrective factor H_C is calculated from the intersection of the best fit curves (straight lines) with the H axis.

TABLE III. Wladoil SAE 90 measurement conditions and viscosity.

Measurement conditions	
Fluid temperature	25 °C.
Pressure	1005 mbars
Viscosity (nominal value)	377.5 mPa s
Results	
Corrective factor (H_c)	2.5 ± 0.4 mm
Measured viscosity	378.6 ± 3.7 mPa s.
Relative difference on viscosity nominal value	0.3%

In the developed device an automatic control of the fluid temperature has not been designed yet, nevertheless motor has been driven by voltage steps, as shown in Figure 6, in order to limit the temperature increase. Besides that, with the purpose to limit further variations in the fluid temperature as well as vibrations produced by the motor, measurements have been carried out with a rotor speed that does not exceed 50% of the corresponding maximum motor speed, checking at the end of every measurement cycle, if temperature fluctuations do

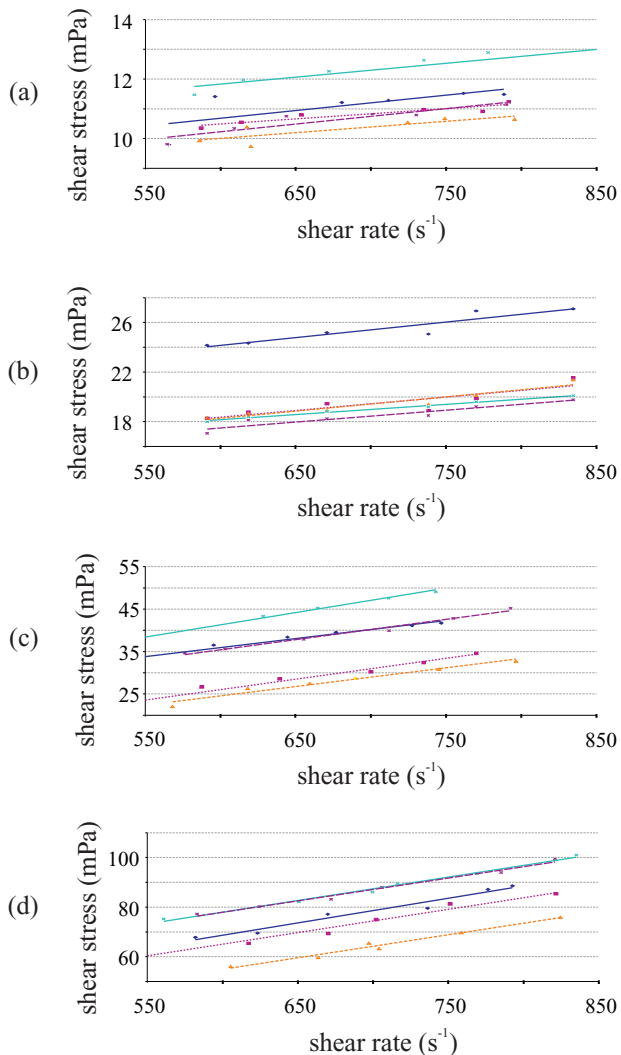


FIG. 8. Rheological curves for four different certified fluids. Different styles refer to different measurement data sets: in (a) nominal viscosity of the reference fluid is 4.80 mPa s, in (b) 9.60 mPa s, in (c) 47.6 mPa s, and in (d) 98.0 mPa s.

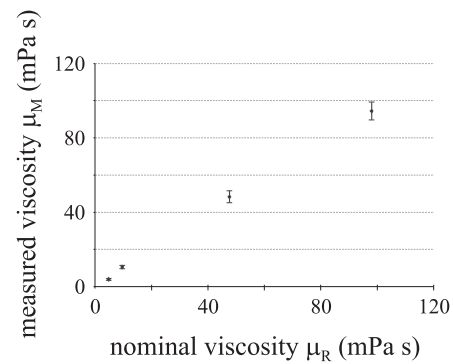


FIG. 9. Calibration results: measured viscosity of the reference fluids versus nominal viscosity.

not exceed ± 2 °C. In Fig. 8 some rheological curves for each reference fluid described in Table II are plotted, whereas in Figure 9 and Table IV calibration results are shown. The measurement uncertainty has been evaluated on 5 data sets from the same fluid (each data set is made up by pairs of τ and γ values, acquired at increasing steps of the rotor speed); for each data set viscosity has been evaluated from the angular coefficient of the best fit straight line (Newtonian fluid). Subsequently, for each fluid a mean viscosity is calculated, and the dispersion of the data around the mean is expressed with a 95% confidence level.

In Fig. 10(a) the rheometer calibration curve is plotted, whereas in Figure 10(b) relative errors from the nominal viscosity μ_R are shown for each certified fluid, calculated as $(\mu_M - \mu_R)/\mu_R \cdot 100$, where μ_M is the mean viscosity, evaluated from the mean of the viscosity values measured by the developed system for each data set. As shown in Fig. 9 and Table IV, measurement results are affected by a relative uncertainty below 10%, depending on the viscosity value μ_M : the uncertainty slightly decreases for increasing μ_M values. In particular for higher μ_M values the relative difference $(\mu_M - \mu_R)/\mu_M$ between measured and nominal values decreases from about 25%–4% for 4.80 mPa s and 98.0 mPa s, respectively. That behavior can be due to inevitable mechanical resistances and skews that are more influent at low viscosity and lead to worse precision and accuracy in measurements. Therefore the system is suitable for viscosity measurement from 1 mPa s to 100 mPa s with an accuracy below the 5% of full scale range. Further measurements have been carried out on two oils with known characteristics to verify instrument behavior, Shell X100 ($\mu_R = 184.5$ mPa s) and Wladoil SAE 90 ($\mu_R = 377.5$ mPa s): results show a relative error below 2.4% for both of them.

TABLE IV. Calibration results at 25 °C.

μ_R (mPa s)	μ_M (mPa s)	Uncertainty on μ_M (mPa s)	Relative uncertainty on μ_M (%)
4.80	3.9	± 0.4	± 10.2
9.60	10.6	± 0.9	± 8.5
47.6	43	± 3	± 7.0
98.0	94	± 5	± 5.3

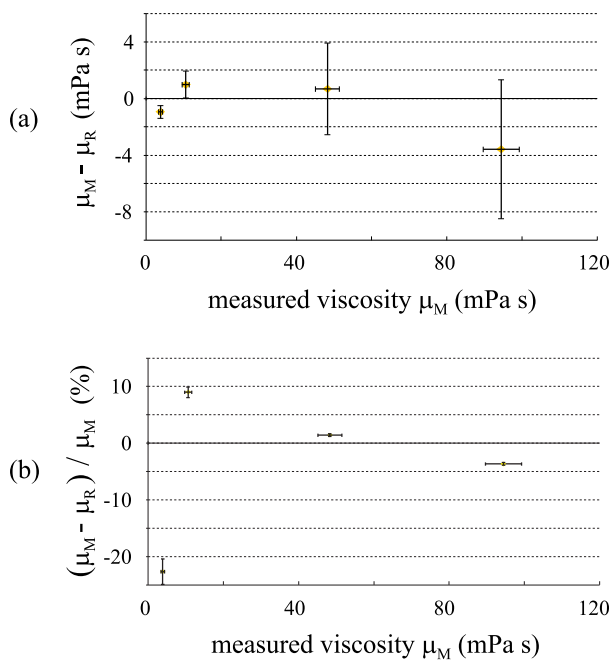


FIG. 10. Rheometer calibration curve and relative error for four different certified fluids. In (a) difference between measured and nominal value, in (b) relative error versus measured viscosity.

IV. CONCLUSIONS

In this work a low cost rheometer for biological fluids has been developed and tested. The device is a coaxial-cylinders type and allows to determine the experimental law between shear stress τ and shear rate $\dot{\gamma}$. In particular, the system is used to measure the viscosity of small volumes of fluid from

1 mPa s to 100 mPa s, with an accuracy below the 5% of full scale range. Results seem to be suitable for measurements on biological fluids. In particular, in the next future, after a full characterization of the device and the development of a fluid temperature control system, measurements on human bone marrow are going to be planned to test biological models and support clinical studies.

¹A. Komoda, Y. Hirooka, K. Miyachi, T. Yoshihara, A. Matsuda, H. Yasunaga, and H. Kimura, *Kawasaki Steel Technical Report* **8**, 17–27 (1983).

²J. Ashmore, A. Q. Shen, H. P. Kavehpour, H. A. Stone, and G. H. McKinley, *J. Eng. Math.* **60**(1), 17–41 (2008).

³C. De Marchis, M. Schmid, and S. Conforto, *Med. Eng. Phys.* **34**(9), 1268–1277 (2012).

⁴M. M. Steinborn, A. F. Heuck, R. Tiling, M. Bruegel, L. Gauger, and M. F. Reiser, *J. Comput. Assist. Tomogr.* **23**(1), 123–129 (1999).

⁵C. W. Macosko, *Rheology, Principles, Measurements and Applications* (Wiley, NY, 1994), p. 568.

⁶D. Bell, *Phys. Ed.* **14**, 432 (1979).

⁷Y. Y. Hou and H. O. Kassim, *Rev. Sci. Instrum.* **76**, 101101 (2005).

⁸A. Y. Malkin and A. I. Sayev, *Rheology Concepts, Methods, and Applications*, 2nd ed. (ChemTec Publishing, Toronto, 2012), p. 528.

⁹M. A. Rao, *Rheology of Fluid and Semisolid Foods Principles and Applications* (Aspen Publishers, Maryland, 1999), p. 433.

¹⁰U. A. Gurkan and O. Akkus, *Ann. Biomed. Eng.* **36**(12), 1978–1991 (2008).

¹¹C. F. Ferraris, *J. Res. Natl. Inst. Stand. Technol.* **104**(5), 461 (1999).

¹²DIN 53019-1:2008-09, “Viscometry – Measurement of Viscosities and Flow Curves by Means of Rotational Viscometers – Part 1: Principles and Geometry of Measuring System.”

¹³G. I. Taylor, *Philos. Trans. R. Soc. London A* **223**, 289 (1923).

¹⁴Z. Zhong and O. Akkus, *Biorheology* **48**, 89–97 (2011).

¹⁵T. Kotaka, D. Ito, H. Kikura, M. Aritomi, and H. Shuichiro, in *Proceedings of the Fifth International Symposium on Ultrasonic Doppler Methods for Fluid Mechanics and Fluid Engineering, Zurich, Switzerland, 12–14 September 2006, Laboratory of Food Process Engineering* (Institute of Food Science and Nutrition, ETH Zurich, Switzerland, 2006), pp. 93–96.